Sato J, Akahane M, Inano S, Terasaki M, Akai H, Katsura M, Matsuda I, Kunimatsu A, Ohtomo K.	Effect of radiation dose and adaptive statistical iterative reconstruction on image quality of pulmonary computed tomography.	Jpn J Radiol	30(2)	146-53	2012
Tomizawa N, Komatsu S, Akahane M, Torigoe R, Kiryu S, Ohtomo K	Relationship between beat to beat coronary artery motion and image quality in prospectively ECG-gated two heart beat 320-detector row coronary CT angiography.	Int J Cardiovasc Imaging	28(1)	139-46	2012
Tomizawa N, Nojo T, Akahane M, Torigoe R, Kiryu S, Ohtomo K.	Adaptive Iterative Dose Reduction in coronary CT angiography using 320-row CT:assessment of radiation dose reduction and image quality.	J Cardiovasc Comput Tomogr	6(5)	318-24	2012
Kurita M, Okazaki M, Kaminishi-Tanikawa A, Niikura M, Takushima A, HariiK.	Differential expression of wound fibrotic factors between facial and trunk dermal fibroblasts.	Connect Tissue Res	53	349-54	2012
Aini H, Ochi H, Iwata M, Okawa A, Koga D, Okazaki M, Sano A, Asou Y.	Procyanidin B3 prevents articular cartilage degeneration and heterotopic cartilage formation in a mouse surgical osteoarthritis model.	PLoS One	7	e37728	2012
新田尚隆	Elasticity evaluation of regenerating cartilage sample based on laser Doppler measurement of ultrasonic particle velocity.	Jpn J Appl Phys	51(7)	07GF15-1-8	2012

Biomedical Research 33 (5) 281-289, 2012

Application of floating cells for improved harvest in human chondrocyte culture

Kazumichi YONENAGA[1, 2], Satoru NISHIZAWA[1], Yuko FUJIHARA[1], Yukiyo ASAWA[1], Sanshiro KANAZAWA[1], Satoru NAGATA[3], Tsuyoshi TAKATO[2], and Kazuto HOSHI[1]

Departments of [1] Cartilage & Bone Regeneration (Fujisoft), and [2] Sensory & Motor System, Graduate School of Medicine, The University of Tokyo, Hongo 7-3-1, Bunkyo-ku, Tokyo 113-8655, Japan; [3] Nagata Microtia and Reconstractive Plastic Surgery Clinic, Sasameminamicho 22-1 Totsuka, Saitama 335-0035, Japan

(Received 22 June 2012; and accepted 30 July 2012)

ABSTRACT

Cell culture medium, which must be discarded during medium change, may contain many cells that do not attach to culture plates. In the present study, we focused on these floating cells and attempted to determine their usefulness for cartilage regeneration. We counted the number of floating cells discarded during medium change and compared the proliferation and differentiation between floating cells and their adherent counterparts. Chondrocyte monolayer culture at a density of 5×10^3 cells/cm^2 produced viable floating cells at a rate of $2.7–3.2 \times 10^3$ cells/cm^2 per primary culture. When only the floating cells from one dish were harvested and replated in another dish, the number of cells was 2.8×10^4 cells/cm^2 (approximately half confluency) on culture day 7. The number of cells was half of that obtained by culturing only adherent cells (5×10^4 cells/cm^2). The floating and adherent cells showed similar proliferation and differentiation properties. The recovery of floating cells from the culture medium could provide an approximately 1.5-fold increase in cell number over conventional monolayer culture. Thus, the collection of floating cells may be regarded as a simple, easy, and reliable method to increase the cell harvest for chondrocytes.

Research on cartilage regeneration is relatively advanced compared with that on other tissues, and some protocols have already been applied in clinical settings. Autologous chondrocytes have been implanted in patients with focal cartilage defects in their joints since as early as the 1990s (4), and these cells have been used for nasal augmentation by injection into subcutaneous pockets (31). It is important for further progress in cartilage regeneration to increase the number of chondrocytes that can be harvested.

Physiologically, chondrocytes proliferate and multiply even when surrounded by solid extracellular matrix in all directions. Thus, cartilage expands by means of interstitial growth *in vivo* (2, 5). However, once chondrocytes are isolated from native tissue and begin to multiply in culture, they inevitably lose their ability to produce cartilaginous matrix components such as glycosaminoglycans (GAG) and type II collagen (COL2), and they begin to produce type I collagen (COL1) in a process termed dedifferentiation (3). The prevention of dedifferentiation in cultured chondrocytes and the redifferentiation of dedifferentiated cells are issues to be solved in the cytological fields (17).

To prevent excessive dedifferentiation, a sufficient number of chondrocytes should be obtained to permit minimal multiplication of cells because an increase in the number of cell passages performed reduces the capacity of the chondrocytes for differentiation or cartilage regeneration *in vivo* (6, 30).

Address correspondence to: Kazuto Hoshi, M.D., Ph.D.
Department of Cartilage & Bone Regeneration (Fujisoft), Graduate School of Medicine, The University of Tokyo, Hongo 7-3-1, Bunkyo-ku, Tokyo 113-8655, Japan
Tel: +81-3-3815-5411 (ext. 37386), Fax: +81-3-5800-9891
E-mail: pochi-tky@umin.net

Long-term culture with repeated passaging also increases the risk of bacterial infection or cross-contamination of cells from other donors. Shortening the culture period may benefit patients by reducing the therapy period, thereby improving quality of life and health (8).

We attempted to improve the efficacy of collagenase digestion for chondrocyte isolation from cartilage and to harvest the maximum possible number of viable cells (34). With this method, we successfully obtained 1×10^7 viable cells/g from the tissue, which was approximately 10-fold higher than the value previously reported (1×10^6 cells/g) (15). We seeded cells at a low cell density (5,000 cells/cm^2), which improved the efficacy of cell expansion and suggests that the actual gain would be increased by more than 1 order of magnitude. However, we often observed cells that did not adhere to culture plates and continued to float over a certain time period after cell seeding. In general, we changed the culture medium every 2 or 3 days (23, 24), at which time these floating cells were generally discarded.

We reasoned that if adequate space is provided for the attachment of cells, the cells floating within the medium may effectively adhere to the plate and begin to proliferate. Thus, in the present study, we focused on the non-adherent cells in the cell culture medium. We examined the characteristics of these floating cells and discuss the possibility of using them in clinical applications.

MATERIALS AND METHODS

Cell isolation and monolayer culture. All procedures were approved by the Ethics Committee of the University of Tokyo Hospital (ethics permission number 622). Remnant auricular cartilage from 3 microtia patients was obtained during surgery in compliance with the Helsinki Principles. The chondrocytes were isolated by digestion with 0.3% collagenase over 24 h (Wako Pure Chemical Industries, Osaka, Japan). The primary auricular chondrocytes were seeded in 35-mm collagen type I-coated plastic culture dishes (n = 36) at a density of 5×10^3 cells/cm^2 and cultured in 2 mL of Dulbecco's modified Eagle's medium/F12 (DMEM/F12) containing 5% human serum supplemented with fibroblast growth factor-2 (100 ng/mL) and insulin (5 μg/mL) as previously described (10, 22).

We divided the 36 dishes into 3 groups (n = 12 per group). The media were changed at different times (day 1, 2, or 3 of culture) in each group. Floating cells, which are usually discarded, were collected from the media (Fig. 1). The samples from each day were further divided into 2 subgroups: centrifugation and non-centrifugation. In the centrifugation group ($430 \times g$ for 5 min), the supernatants were discarded before seeding. The cells were counted using a NucleoCounter (ChemoMetec, Allerod, Denmark) (35). In contrast, the entire cell suspension was used for seeding in the non-centrifugation group. The cells obtained from 1, 2, or 3 dishes of primary cultures were combined into another, separate dish. Floating cells were cultured in a monolayer and then harvested at day 7, at which time the adherent cells had also reached confluence. Harvested cells were divided into three groups: adherent cells only (A), floating cells only (F), and mixed cell culture, in which the numbers of adherent and floating cells were equal (F + A) (Fig. 1). These cells were reseeded at a density of 2.5×10^3 cells/cm^2 and then incubated for 1 week, at which time the gene expression of type I collagen αI chain (COL1A1) and type II collagen αI chain (COL2A1) was evaluated. We used trypsin-EDTA solution to lift the cells during subculturing.

Pellet culture. For the pellet culture, cultured chondrocytes were suspended in 0.8% atelocollagen solution (Kawaken Fine Chemicals, Tokyo, Japan) at a density of 10^7 cells/mL. The atelocollagen pellets were cultured in DMEM/F12 medium with soluble factors for 3 weeks. We used recombinant human bone morphogenetic protein-2 (rhBMP-2, kindly provided by Astellas Pharma, Tokyo, Japan), rh-insulin (MP Biomedicals, Irvine, CA), and L-3, 3', 5-triiodothyronine (T3, EMD Bioscience). The dosage of each factor was determined to be 200 ng/mL BMP-2, 5 μg/mL insulin, and 100 nmol/L T3 on the basis of our and other previous reports (7, 9, 11, 12, 14, 16, 18, 21, 28, 36).

Real-time reverse transcription-polymerase chain reaction analysis. Total RNA was isolated from the chondrocytes with ISOGEN (Wako Pure Chemical Industries) according to the manufacturer's protocol. Complementary DNA (cDNA) was synthesized from 1 μg of total RNA using the Superscript II reverse transcriptase kit (Invitrogen, Carlsbad, CA). The cDNA of the target genes, including the PCR amplicon sequences, was amplified by PCR and used as standard templates after linearization. A QuantiTect SYBR Green PCR Master Mix (Qiagen, Hilden, Germany) was used, and SYBR Green PCR amplification and real-time fluorescence detection were performed with the ABI 7700 sequence detection

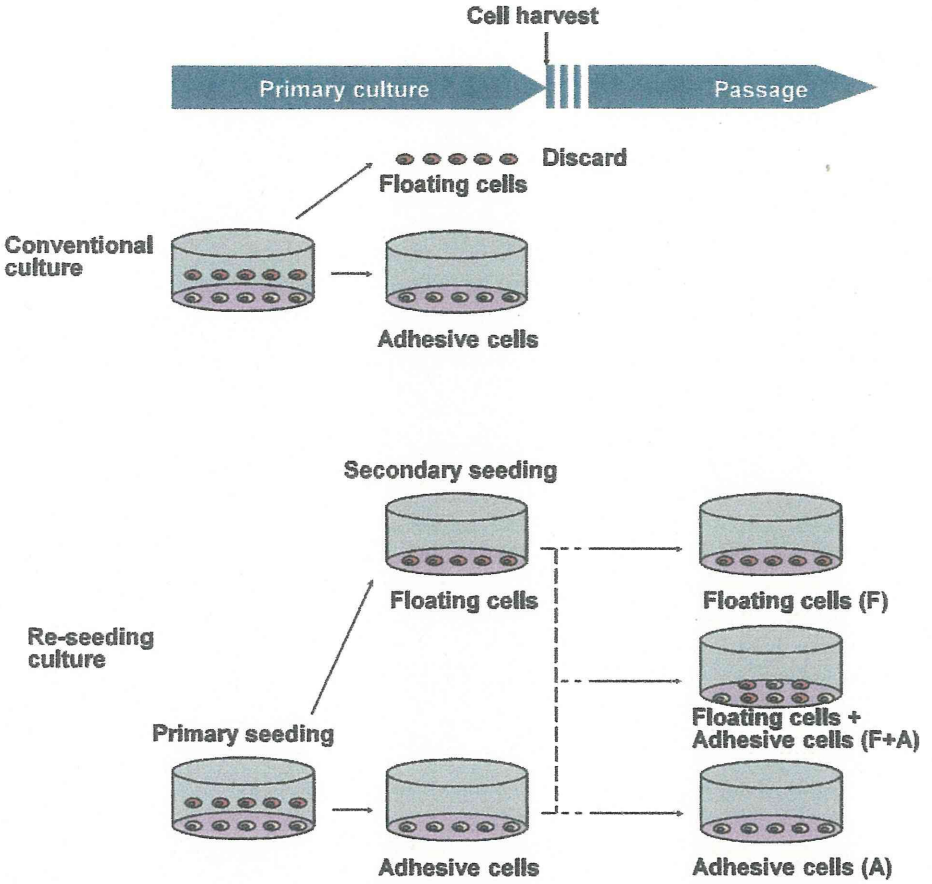

Fig. 1 Experimental design. **(Upper)** In conventional culture, we discarded the floating cells. **(Lower)** In this experiment, floating cells were collected from the media for reseeding culture. On day 7 of culture, we subcultured the cells under three conditions: only floating cells (F), both floating cells and adherent cells (F + A), and only adherent cells (A).

system. All reactions were run in quadruplicate. The sequences of the primers were 5'-CTCCTCGCTT TCCTTCCTCT-3' and 5'-GTGCTAAAGGTGCCAA TGGT-3' for COL1A1; 5'-GAGTCAAGGGTGATC GTGGT-3' and 5'-CACCTTGGTCTCCAGAAG GA-3' for COL2A1; and 5'-GAAG GTGAAGGTC GGAGTCA-3' and 5'-GAAGATGGTGATGGGAT TTC-3' for glyceraldehyde-3-phosphate dehydrogenase (GAPDH).

GAG measurement. The sulfated GAG content was measured using an Alcian blue binding assay (Wieslab AB, Lund, Sweden). After digestion of the chondrocyte-containing atelocollagen pellet in 0.3% collagenase for 1 h at 37°C, the cell debris and insoluble material were removed by centrifugation at 6,000 × *g* for 30 min. GAG in the supernatant was precipitated using Alcian blue solution, and the sediments were redissolved in 4 mol/L GuHCl-33% propanol solution by centrifugation at 6,000 × *g* for 15 min. The spectrophotometric absorbance of the mixture was measured at 600 nm.

Enzyme-linked immunosorbent assay for COL1 and COL2. Collagen protein levels in the pellets were quantified by an enzyme-linked immunosorbent assay using a human type 1 and type 2 collagen detection kit (Chondrex, Redmond, WA). The pellets were dissolved in 10 mg/mL pepsin and 0.05 M acetic acid at 4°C for 48 h and then incubated in 1 mg/mL pancreatic elastase, 0.1 mmol/L Tris, 0.02 mol/L NaCl, and 5 mmol/L $CaCl_2$ (pH 7.8–8.0) at 4°C overnight. The samples were centrifuged at 9,100 × *g* for 5 min to remove the residue. The collagen proteins were bound by polyclonal anti-human COL1 or COL2 antibodies (Chondrex) and detected by biotinylated secondary antibodies and streptavidin peroxidase. *o*-Phenylenediamine and H_2O_2 were added to the mixture, and the spectrophotometric absorbance of the mixture was measured at 490 nm.

Histology. The regenerated cartilage was fixed with 4% paraformaldehyde, embedded in optimal cutting temperature (OCT) compound (Sakura, Tokyo, Japan), and cryosectioned into 10-μm-thick slices. The sections were stained with toluidine blue O.

RESULTS

Viable floating cells from day 1, 2, or 3 of culture were harvested in amounts ranging from 2.7×10^3 to 3.2×10^3 cells/cm^2, with no significant differences observed among the groups. The floating cells were counted constantly regardless of the harvested period within 3 days (Fig. 2). We harvested the floating cells on day 1, 2, or 3 and transferred them to new dishes with or without centrifugation (Fig. 3). Regardless of whether the floating cells were removed from the primary culture on day 1, 2, or 3, the number of adherent cells remaining in the primary cultures on day 7 was almost identical (approximately 5×10^4 cells/cm^2) in each group (Fig. 3 and Fig. 4A). For the reseeding of floating cells, centrifugation before seeding appeared to improve cell adhesion and proliferation (Fig. 3).

On day 7 of culture, the number of floating cells harvested from one dish on day 1 and reseeded on one culture dish reached approximately 2.8×10^4 cells/cm^2, whereas the number of floating cells combined from two dishes reached 4.2×10^4 cells/cm^2, and that from three dishes reached 4.8×10^4 cells/cm^2. These values were similar when the floating cells were harvested and reseeded on day 2, but they clearly decreased and were below the limit of detection for counting when the cells were harvested and reseeded on day 3 of culture (Fig. 4B). Thus, the number of cells reached a maximum when the cells harvested from one original dish on day 1 of culture were reseeded onto a new dish (Fig. 4C).

We next examined the properties of the regenerated cartilage containing floating cells and/or adherent cells (Fig. 5). Chondrocytes were embedded in 0.8% atelocollagen gel at a density of 10^7 cells/mL. We used RT-PCR to examine the expression of COL1A1 and COL2A1 in cultured human auricular chondrocytes embedded in these three-dimensional matrices after 1 week. No significant differences were observed among groups containing floating cells and adherent cells in different ratios (Fig. 5). At 3 weeks, the sizes of the pellets were almost identical in all of the groups (Fig. 6A, *Upper*), and histological analyses using toluidine blue O staining revealed similar accumulation of proteoglycan (Fig. 6A, *Lower*). The levels of COL2 and GAG, both of which

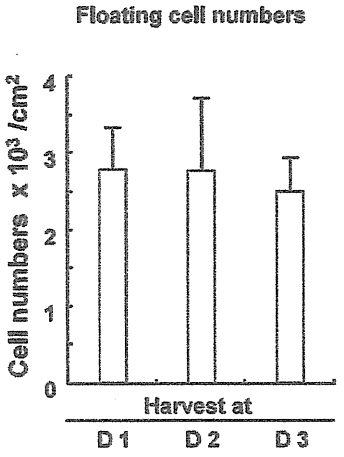

Fig. 2 The number of viable floating cells on day 1, 2, or 3 of culture before reseeding was not significantly different. All values are presented as the mean and standard deviation of three samples per group.

are specific components of cartilaginous tissues, were equivalent in regenerated cartilage produced by floating cells and adherent cells, and the levels of COL1 were comparable across groups (Fig. 6B).

DISCUSSION

The results presented here indicate that the proliferation capacity of floating cells is the same as that of adherent cells. We postulate that the initially nonadherent cells represent the population of cells that did not have adequate space to adhere in primary cultures. Cells may also become less adherent during cell division (19). During this period, some cells detach from the culture dishes, possibly becoming floating cells. The floating cells may be continuously produced, even after primary culture.

With centrifugation before reseeding, *i.e.*, before the medium change, the cells strongly adhered to the plates and began to proliferate, as shown in Fig. 3. This may have been caused by some collagenase remaining in the medium of the primary culture when the washing step performed after enzymatic digestion was not sufficient. High concentrations and long incubation periods with collagenase are cytotoxic, as shown in a previous study (34). Another explanation for our observation is that a shortage of nutrition or growth factors may have occurred because of the decrease in the number of medium changes, which may have reduced the cell viability and adhesion of the chondrocytes. Therefore, although frequent medium changes with centrifugation may increase the risk of cell loss during

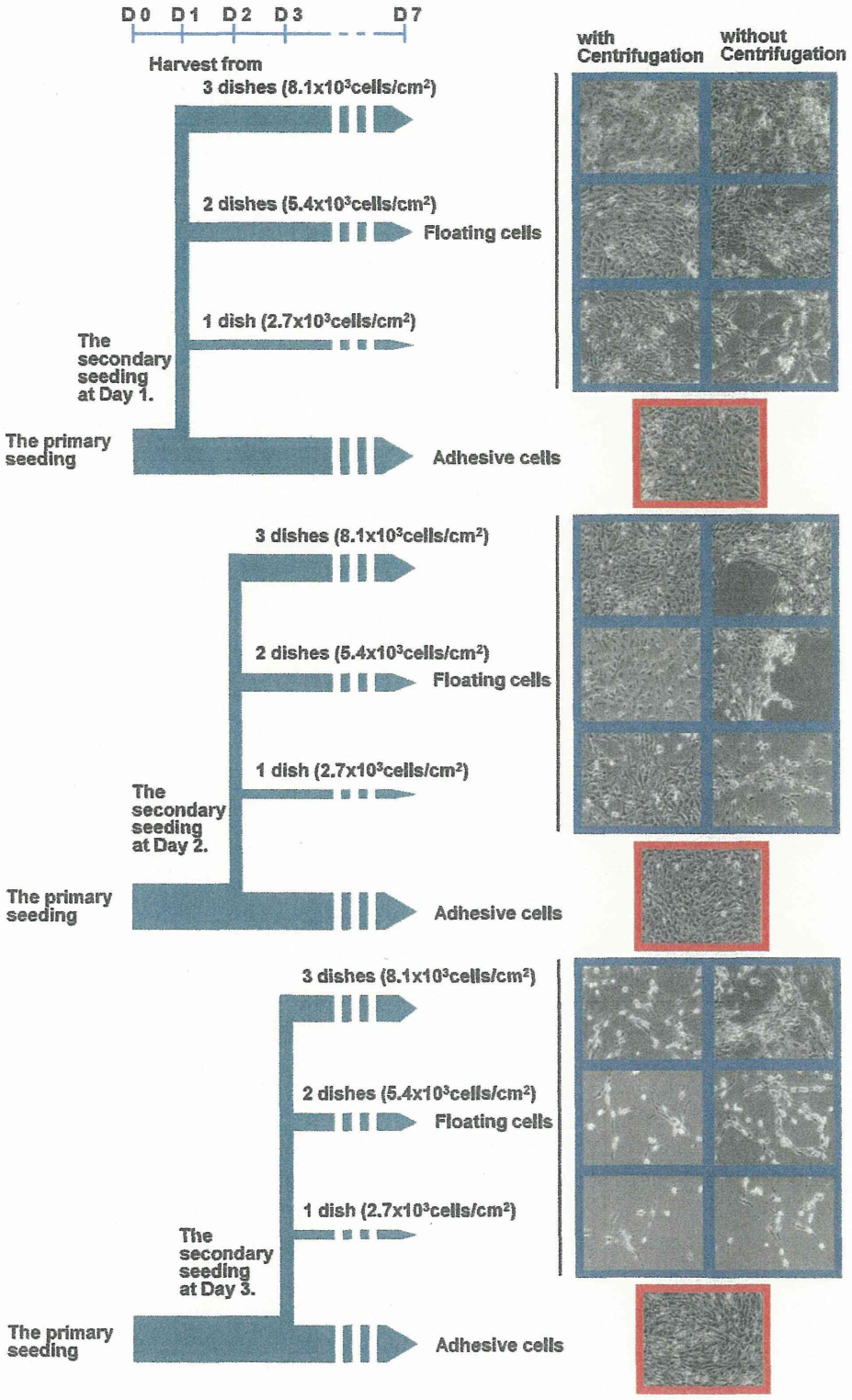

Fig. 3 Phase-contrast images obtained upon reseeding of floating cells. The floating cells harvested from 1, 2, or 3 dishes were plated on a new dish with or without centrifugation. Regardless of whether floating cells were removed from the primary culture on day 1, 2, or 3, the number of adherent cells remaining in the primary culture dish on day 7 was almost identical across groups (red squares). Centrifugation before reseeding improved the adhesion and proliferation of floating cells (blue square).

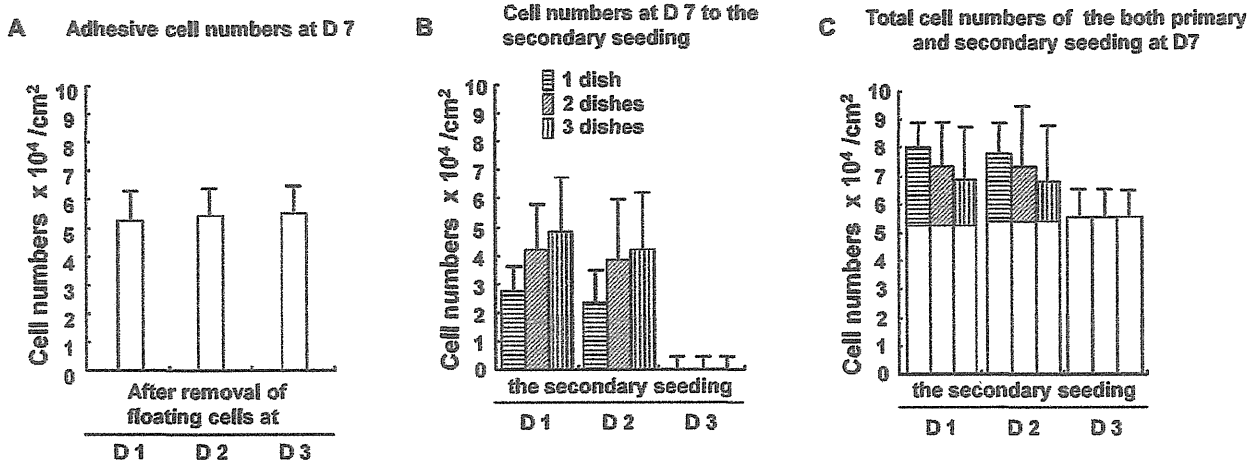

Fig. 4 The number of cells on day 7 of culture. (A) The conventionally cultured chondrocytes reached a density of approximately 5×10^4 cells/cm^2 regardless of whether the floating cells were harvested on day 1, 2, or 3 of culture. (B) On day 7 of culture, cells from a dish that had been reseeded on day 1 numbered approximately 2.8×10^4 cells/cm^2, cells combined from two dishes numbered 4.2×10^4 cells/cm^2, and cells combined from three dishes numbered 4.8×10^4 cells/cm^2; the numbers were similar for cells reseeded on day 2. However, cells reseeded on day 3 were markedly reduced in number on day 7 of culture. (C) The maximum number of cells was recovered when the floating cells obtained from one dish on day 1 of culture were reseeded on one new dish. All values are presented as the mean and standard deviation of three samples per group.

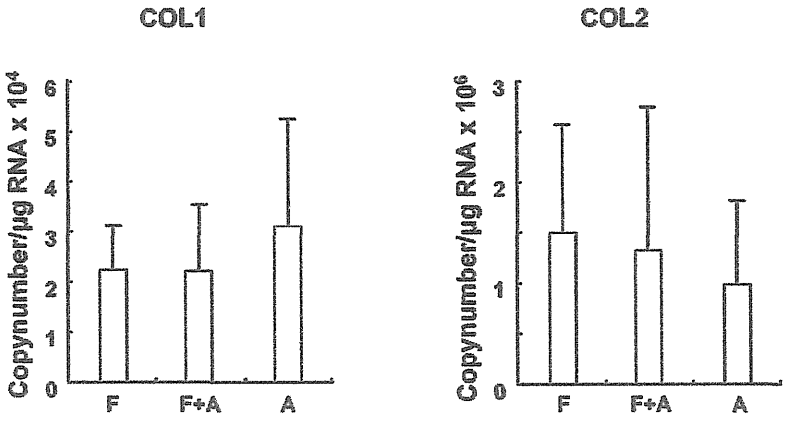

Fig. 5 COL1A1 and COL2A1 mRNA levels measured by real-time RT-PCR after 1 week of pellet culture did not significantly differ among pellets consisting of only floating cells (F), both floating cells and adherent cells (F + A), and only adherent cells (A). All values are presented as the mean and standard deviation of three samples per group.

cell passaging, a medium change is required before the reseeding of floating cells.

The number of cultured floating cells prominently decreased when the cells were harvested and reseeded on day 3 of culture (Fig. 4B), possibly because a culture time of only 4 days was insufficient. Thus, we could not accurately count the cells using the NucleoCounter (35).

The COL2 evaluated in this study is a specific cartilage component. COL2 forms fibrils that permit cartilage to entrap proteoglycan aggregates and impart tensile strength to the tissue. Aggrecan is a cartilage-specific proteoglycan whose levels are elevated in cartilaginous regions where COL2 is also present (27). Because repeated passaging decreased the COL2 level and cell proliferation (26), it is preferable to minimize the passaging of the cells to preserve their physiological function.

Every laboratory engaged in the research and development of biomedical applications utilizes various unique protocols to provide three-dimensional structures (13, 20, 25). Future directions include the

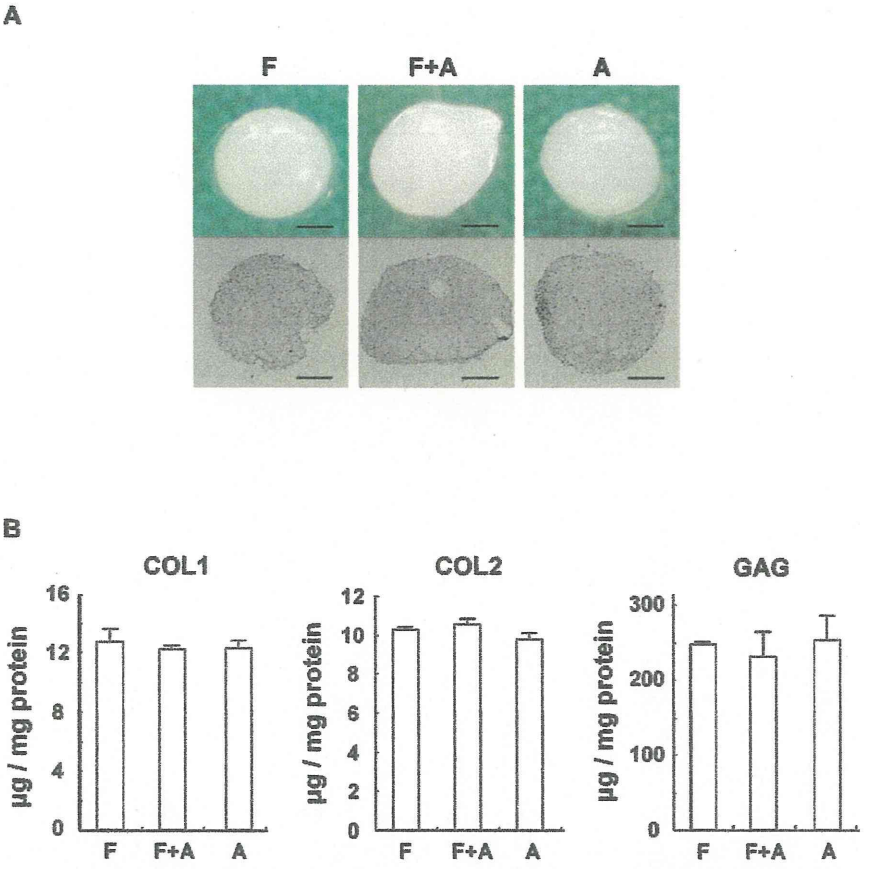

Fig. 6 Histological and biochemical analyses of regenerated cartilage pellets. (**A**) Macroscopic (Upper) and histological findings with toluidine blue O staining (Lower) after 3 weeks of pellet culture. Scale bars, 1 mm. (**B**) COL1, COL2, and GAG protein levels after 3 weeks of pellet culture. No significant differences were observed between the three groups, *i.e.*, floating cells only (F), both floating cells and adherent cells (F + A), and adherent cells only (A). All values are presented as the mean and standard deviation of three samples per group.

manufacture of regenerated cartilage with a three-dimensional structure and a size of $5 \times 0.5 \times 0.5$ cm^3 for the correction of congenital nasal deformities (1). At least 1×10^8 cells will be necessary for the production of regenerated cartilage of this size. Based on the results of a previous report regarding the concentration of collagenase required for digestion and the cell density at seeding, we consistently collected 1×10^6 cells from approximately 0.1 g of biopsied cartilage (34). When we seeded these cells at a density of 3,000–10,000 cells/cm^2, we obtained over 1×10^7 cells at the end of the primary culture and reached the goal of over 1×10^8 cells on the subsequent passage. If the floating cells are recovered from culture, an approximately 1.5-fold increase in the cell number can be achieved. Thus, the volume of biopsied tissue (for example, original weight 0.1 g) can be decreased by one-third (0.067 g), and the application of this novel method may reduce the surgical invasiveness of the biopsy and the physical strain on patients (22, 29, 31, 32).

Minimal invasiveness is one of the major goals of biomedical techniques, and our method may increase the advantages of this approach (33). Moreover, if this culture method can be used not only for primary cultures but also for subcultures, it may permit large quantities of cultured cells to be obtained in a short time. This method could be applied to various cell culture systems and may be commonly used as a key biomedical technique.

Acknowledgements

We thank Mr. Takashi Nakamoto, Ms. Miki Akizawa, Mr. Motoki Yagi, Mr. Tomoaki Sakamoto, and Mr. Makoto Watanabe for technical support. This work was supported by Grants-in-Aid for Scientific Research from the Ministry of Education, Culture,

Sports, Science and Technology of Japan (MEXT, No. 21390532 and 21659462), and Research and Development Programs for Three-dimensional Complex Organ Structures from the New Energy and Industrial Technology Development Organization and for Resolving Critical Issues from Special Coordination Funds for Promoting Science and Technology (SCF) commissioned by MEXT.

REFERENCES

1. Asawa Y, Ogasawara T, Takahashi T, Yamaoka H, Nishizawa S, Matsudaira K, Mori Y, Takato T and Hoshi K (2009) Aptitude of auricular and nasoseptal chondrocytes cultured under a monolayer or three-dimensional condition for cartilage tissue engineering. *Tissue Eng Part A* **15**, 1109–1118.
2. Bakker VM and Johnston LE Jr (1985) The effect of Class II elastic forces on craniofacial growth in rats. *J Dent Res* **64**, 44–47.
3. Benya PD (1981) Two-dimensional CNBr peptide patterns of collagen types I, II and III. *Coll Relat Res* **1**, 17–26.
4. Brittberg M, Lindahl A, Nilsson A, Ohlsson C, Isaksson O and Peterson L (1994) Treatment of deep cartilage defects in the knee with autologous chondrocyte transplantation. *N Engl J Med* **331**, 889–895.
5. Freitas PH, Kojima T, Ubaidus S, Suzuki A, Li M, Yoshizawa M, Oda K, Maeda T, Kudo A, Saito C and Amizuka N (2007) Histochemical examinations on cortical bone regeneration induced by thermoplastic bioresorbable plates applied to bone defects of rat calvariae. *Biomed Res* **28**, 191–203.
6. Fujihara Y, Takato T and Hoshi K (2010) Immunological response to tissue-engineered cartilage derived from auricular chondrocytes and a PLLA scaffold in transgenic mice. *Biomaterials* **31**, 1227–1234.
7. Grigoriadis AE, Aubin JE and Heersche JN (1989) Effects of dexamethasone and vitamin D3 on cartilage differentiation in a clonal chondrogenic cell population. *Endocrinology* **125**, 2103–2110.
8. Jiao Y, Wang D, Han W and Hu J (1999) Phenotypic changes of mandibular condylar cartilage cells during subculture. *Hua Xi Kou Qiang Yi Xue Za Zhi* **17**, 355–357.
9. Kato Y and Gospodarowicz D (1984) Growth requirements of low-density rabbit costal chondrocyte cultures maintained in serum-free medium. *J Cell Physiol* **120**, 354–363.
10. Liu G, Kawaguchi H, Ogasawara T, Asawa Y, Kishimoto J, Takahashi T, Chung UI, Yamaoka H, Asato H, Nakamura K, Takato T and Hoshi K (2007) Optimal combination of soluble factors for tissue engineering of permanent cartilage from cultured human chondrocytes. *J Biol Chem* **282**, 20407–20415.
11. Malinin TI and Hornicek FJ (1997) Response of human chondrocytes cultured in vitro to human somatotropin, triiodothyronine, and thyroxine. *Transplant Proc* **29**, 2037–2039.
12. Maor G, Segev Y and Phillip M (1999) Testosterone stimulates insulin-like growth factor-I and insulin-like growth factor-I-receptor gene expression in the mandibular condyle—a model of endochondral ossification. *Endocrinology* **140**, 1901–1910.
13. Mohan N, Nair PD and Tabata Y (2009) A 3D biodegradable protein based matrix for cartilage tissue engineering and stem cell differentiation to cartilage. *J Mater Sci Mater Med* **20** Suppl 1, S49–S60.
14. Monsonego E, Halevy O, Gertler A, Hurwitz S and Pines M (1995) Growth hormone inhibits differentiation of avian epiphyseal growth-plate chondrocytes. *Mol Cell Endocrinol* **114**, 35–42.
15. Peterson L, Minas T, Brittberg M, Nilsson A, Sjögren-Jansson E and Lindahl A (2000) Two- to 9-year outcome after autologous chondrocyte transplantation of the knee. *Clin Orthop Relat Res* **374**, 212–234.
16. Rodd C, Jourdain N and Alini M (2004) Action of estradiol on epiphyseal growth plate chondrocytes. *Calcif Tissue Int* **75**, 214–224.
17. Schnabel M, Marlovits S, Eckhoff G, Fichtel I, Gotzen L, Vécsei V and Schlegel J (2002) De-differentiation-associated changes in morphology and gene expression in primary human articular chondrocytes in cell culture. *Osteoarthritis Cartilage* **10**, 62–70.
18. Shukunami C, Ohta Y, Sakuda M and Hiraki Y (1998) Sequential progression of the differentiation program by bone morphogenetic protein-2 in chondrogenic cell line ATDC5. *Exp Cell Res* **241**, 1–11.
19. Soule HD and McGrath CM (1986) A simplified method for passage and long-term growth of human mammary epithelial cells. *In Vitro Cell Dev Biol* **22**, 6–12.
20. Tadokoro M, Matsushima A, Kotobuki N, Hirose M, Kimura Y, Tabata Y, Hattori K and Ohgushi H (2012) Bone morphogenetic protein-2 in biodegradable gelatin and β-tricalcium phosphate sponges enhances the in vivo bone-forming capability of bone marrow mesenchymal stem cells. *J Tissue Eng Regen Med* **6**, 253–260.
21. Takahashi T, Ogasawara T, Kishimoto J, Liu G, Asato H, Nakatsuka T, Uchinuma E, Nakamura K, Kawaguchi H, Chung UI, Takato T and Hoshi K (2005) Synergistic effects of FGF-2 with insulin or IGF-I on the proliferation of human auricular chondrocytes. *Cell Transplant* **14**, 683–693.
22. Takahashi T, Ogasawara T, Asawa Y, Mori Y, Uchinuma E, Takato T and Hoshi K (2007) Three-dimensional microenvironments retain chondrocyte phenotypes during proliferation culture. *Tissue Eng* **13**, 1583–1592.
23. Tanaka Y, Ogasawara T, Asawa Y, Yamaoka H, Nishizawa S, Mori Y, Takato T and Hoshi K (2008) Growth factor contents of autologous human sera prepared by different production methods and their biological effects on chondrocytes. *Cell Biol Int* **32**, 505–514.
24. Tanaka Y, Yamaoka H, Nishizawa S, Nagata S, Ogasawara T, Asawa Y, Fujihara Y, Takato T and Hoshi K (2010) The optimization of porous polymeric scaffolds for chondrocyte/atelocollagen based tissue-engineered cartilage. *Biomaterials* **31**, 4506–4516.
25. Uchiyama H, Yamato M, Sasaki R, Sekine H, Yang J, Ogiuchi H, Ando T and Okano T (2011) In vivo 3D analysis with micro-computed tomography of rat calvaria bone regeneration using periosteal cell sheets fabricated on temperature-responsive culture dishes. *J Tissue Eng Regen Med* **5**, 483–490.
26. Veilleux NH, Yannas IV and Spector M (2004) Effect of passage number and collagen type on the proliferative, biosynthetic, and contractile activity of adult canine articular chondrocytes in type I and II collagen-glycosaminoglycan matrices in vitro. *Tissue Eng* **10**, 119–127.
27. Watanabe H, Yamada Y and Kimata K (1999) Roles of aggrecan, a large chondroitin sulfate proteoglycan, in cartilage structure and function. *J Biochem* **124**, 687–693.
28. Wroblewski J and Edwall-Arvidsson C (1995) Inhibitory effects of basic fibroblast growth factor on chondrocyte differentiation. *J Bone Miner Res* **10**, 735–742.

29. Yamaoka H, Tanaka Y, Nishizawa S, Asawa Y, Takato T and Hoshi K (2010) The application of atelocollagen gel in combination with porous scaffolds for cartilage tissue engineering and its suitable conditions. *J Biomed Mater Res A* **93**, 123–132.
30. Yamaoka H, Asato H, Ogasawara T, Nishizawa S, Takahashi T, Nakatsuka T, Koshima I, Nakamura K, Kawaguchi H, Chung UI, Takato T and Hoshi K (2006) Cartilage tissue engineering using human auricular chondrocytes embedded in different hydrogel materials. *J Biomed Mater Res A* **78**, 1–11.
31. Yanaga H, Yanaga K, Imai K, Koga M, Soejima C and Ohmori K (2006) Clinical application of cultured autologous human auricular chondrocytes with autologous serum for craniofacial or nasal augmentation and repair. *Plast Reconstr Surg* **117**, 2019–2030.
32. Yanaga H, Imai K, Fujimoto T and Yanaga K (2009) Generating ears from cultured autologous auricular chondrocytes by using two-stage implantation in treatment of microtia. *Plast Reconstr Surg* **124**, 817–825.
33. Yokoi M, Hattori K, Narikawa K, Ohgushi H, Tadokoro M, Hoshi K, Takato T, Myoui A, Nanno K, Kato Y, Kanawa M, Sugawara K, Kobo T and Ushida T (2012) Feasibility and limitations of the round robin test for assessment of in vitro chondrogenesis evaluation protocol in a tissue-engineered medical product. *J Tissue Eng Regen Med* **6**, 550–558.
34. Yonenaga K, Nishizawa S, Akizawa M, Asawa Y, Fujihara Y, Takato T and Hoshi K (2010) The optimal conditions of chondrocyte isolation and its seeding in the preparation for cartilage tissue engineering. *Tissue Eng Part C* **16**, 1461–1469.
35. Yonenaga K, Nishizawa S, Akizawa M, Asawa Y, Fujihara Y, Takato T and Hoshi K (2010) Utility of NucleoCounter for the chondrocyte count in the collagenase digest of human native cartilage. *Cytotechnology* **62**, 539–545.
36. Yasuda T and Poole AR (2002) A fibronectin fragment induces type II collagen degradation by collagenase through an interleukin-1-mediated pathway. *Arthritis Rheum* **46**, 138–148.

頭頸部外科　22 (2)：121～124，2012

顎顔面領域における骨軟骨再生医療の現状と展望

高戸　毅[1)]　星　和人[2)]　藤原夕子[2)]
西條英人[1)]　菅野勇樹[1)]　大久保和美[1)]
鄭　雄一[3)]　森　良之[1)]

要旨：顎顔面領域は四肢骨に比較して荷重負荷がかかりにくく，概して再建で必要とされる組織量も少ないことから，再生組織の移植に適した領域であると考えられる。しかし，人工骨や人工歯根など様々な生体材料を用いた治療法が確立しており，また大型の組織欠損に対しては，マイクロサージャリーによる組織再建やエピテーゼによる補綴も行われている。従って，顎顔面領域における再生医療の展開は，既存の医療を低侵襲治療として凌駕する，或いは，より卓越した治療効果を発揮することにより可能になると考える。本稿では，われわれのグループが開発し実用段階に達している骨・軟骨再生医療について，基礎と臨床の面から紹介する。
キーワード：骨軟骨再生医療，顎顔面領域，CT bone，インプラント型再生軟骨

Ⅰ．緒　言

再生医療とは，機能障害や機能不全に陥った生体組織・臓器に対して，細胞を積極的に利用して機能の再生をはかる医療であり，再生医療を利用した新たな治療法の開発に期待が高まっている。

再生医療の歴史は古く，1970年代にまで遡る。1993年には，ハーバード大学医学部子供病院の消化器外科医J P. Vacantiとマサチューセッツ工科大学の応用化学者R. Langerが生分解性高分子製の足場（スカフォールド）に細胞を播種し，成長因子の存在下で組織形成を誘導するというTissue Engineering（組織工学）の概念を提唱した。彼らが提唱する方法で作製されたマウスの背中に乗ったヒトの耳の写真は，世界のマスコミで広く取り上げられ，再生医療を一躍有名にした[1)]。その後，再生医療分野における研究は著しく発展し，ヒト胚性幹細胞（ES細胞），人工多能性幹細胞（iPS細胞）の樹立などが報告された。一方で，本邦で薬事承認を受けた再生医療製品は，現在のところ再生表皮のみであり，世界的に見ても，限局した軟骨欠損に対する再生軟骨が販売されているのみである。Tissue engineeringの提唱から20年を経てなお，実際の臨床で使用可能な再生医療製品の産業化が難航している現状を目の当たりにすると，再生医療の開発認可がいかに困難であるかが窺える。

顎顔面領域は四肢骨に比較して荷重負荷がかかりにくく，概して再建で必要とされる組織量も少ないことから，再生組織の移植に適した領域であると考えられる。とはいえ，既存の治療法である血管柄付骨移植，人工骨や人工歯根など様々な生体材料を用いた治療法，エピテーゼによる補綴などにより，形態的にも良好な組織再建が可能となってきている。従って，顎顔面領域における再生医療の展開は，既存の医療を低侵襲治療として凌駕する，或いは，より卓越した治療効果を発揮することにより可能になると考える。本稿では，われわれのグループが開発し実用段階に達している骨・軟骨再生医療について紹介する。

Ⅱ．In situ tissue engineering

下顎骨再建のfirst choiceとして用いられることが多い血管柄付遊離腓骨移植は，①血行が豊富な長い骨を採取できる，②インプラントを植立するのに十分な太さがある，③頭部操作と並行して，下肢から骨皮弁を採取できる，④皮膚欠損症例に対し，皮膚移植も同時に行える，⑤採取部の合併症が少ないことなどの特長を有している[2)]。しかし，健常部にメスを入れて採骨するために侵襲性は高く，採取できる骨の量と形状には大きな制約がある。また，移植部に適合した形状にするために，術中に移植骨の削合が必要となることが多い。

そこで近年注目を集めているのが，腸骨から採取

[1)] 東京大学医学部附属病院顎口腔外科・歯科矯正歯科
[2)] 東京大学大学院医学系研究科軟骨・骨再生医療寄付講座（富士ソフト）
[3)] 東京大学大学院工学系研究科バイオエンジニアリング専攻
［平成24年3月2日受付，平成24年5月18日受理］

した骨髄海綿骨（particulate cancellous bone and marrow: PCBM）とチタンメッシュトレーによる骨再建法である[3,4]。この方法では，トレーを適切に整形することにより，より自然な形態修復が可能であり，義歯やインプラントなどを併用した良好な咬合回復も期待できる。

PCBM移植では，PCBMに含まれる未分化間葉系由来の細胞による新生骨形成，それに引き続く骨吸収，骨形成により，周囲の母床骨に対応した骨改造が誘導される[5]。つまり，PCBM移植は，自己の骨形成能を利用した，いわゆるin situ tissue engineeringであり，その点において，移植骨そのものの生着を目的とする従来のブロック骨移植や血管柄付き骨移植と根本的に異なっている。また，小顎症の治療で選択される骨延長術も，骨切り部が治癒する過程で生じる仮骨をゆっくりと牽引することにより骨形成を誘導する治療法であり，PCBM移植と同様，in situ tissue engineeringに基づいた治療法であるといえる。このように，再生医療は必ずしも目新しい治療というわけではなく，従来から行われている治療にも，再生医療の概念を利用した治療法が見受けられる。

PCBMとチタンメッシュトレーを用いた手術法の課題として，術後感染の合併があげられる。オトガイ部や下顎枝などを含む再建では，複雑な形態のためトレーの整形が困難であり，皮膚や粘膜の裂開，死腔を生じやすいためであると推察される[4]。将来的には，術前の3Dモデルなどからカスタムメイドのメッシュトレーを作製し，より精度の高い再建を行うことにより安定した治療成績を維持することが可能になると思われる。

Ⅲ．骨再生医療（CT bone）

従来のブロック骨移植や血管柄付き骨移植は，患者自身の健常部から採取するため，移植後の骨癒合も良好で，修復効果も高い。また，チタンメッシュトレーとPCBMを利用した顎骨再建術は，tissue engineeringの概念を利用した骨再生法であり，従来の骨移植法と比較しても多くの利点を有している。しかし，いずれの方法も，自家骨移植であるため採骨部への侵襲は避けられず，採取量にも限界がある。諸外国では，他家骨移植という選択肢もあるが，本邦では，文化的・制度的な背景から普及していない。そこでわれわれは，形状，強度に優れ，且つ分解吸収性がよく，将来的には自己の骨に置換するような人工骨の開発に取り組んできた。

現在，人工骨の主流は，リン酸カルシウムのブロック状多孔体，ペースト，顆粒などである。リン酸カルシウムが頻用される理由としては，骨の一成分であるため生体適合性，生体安全性に優れていること，また，石灰岩とリン鉱石から合成されるため，供給量に制限がないことなどがあげられる[6]。しかし，現段階の人工骨は，強度，形状，操作性，分解吸収・再生誘導能などの機能面において自家骨や他家骨には及ばず，これらの課題を克服する新たな人工骨の開発が求められている。

われわれは，東京大学大学院工学系研究科と連携し，三次元インクジェットプリンターを用いたリン酸三カルシウム粉体積層造形法によるカスタムメイド人工骨（CT bone）の作製を検討してきた[7]。この方法では，リン酸三カルシウム粉体の薄層（0.1 mm）を作り，その上から水を主体とする硬化液をプリントするという過程を繰り返すことにより，外部形状のみならず，内部構造も自由に制御可能な人工骨を作製することができる。大型実験動物を用いた前臨床研究を経て，先天異常，外傷，腫瘍切除などにより非荷重部位に顎顔面変形を有する患者を対象に2006年3月から7月に臨床研究を10例，2008年10月から2009年9月に治験を10例行った（図1）[8]。患者のCT画像をもとに人工骨を作製するため，患部への適合も良好で，術者による形状調整がほぼ不要であった。また，十分な強度を有するため，優れた操作性を示すことも明らかとなった。これまでのところ安全面での問題はなく，人工骨と母骨との癒合も速やかに起こっていることが確認されている。

今後は荷重部への適応拡大を目指し，金属など他材料とのハイブリッド化や骨誘導シグナルとの融合などによる高機能化人工骨の開発が期待される。

Ⅳ．軟骨再生医療（インプラント型再生軟骨）

一般に，軟骨組織は自己修復能に乏しく，いったん障害を受けると自然回復は望めない。従って，関節軟骨損傷などの外傷や変形性関節症などの加齢性疾患，関節リウマチなどの炎症性疾患を患うと，歩行などの生活動作に支障をきたすこととなる。治療としては，人工関節置換術や自家軟骨移植などが行われているが，耐久性，感染，採取部位の侵襲などの課題があり，軟骨再生医療の開発に期待が寄せられている。

軟骨再生医療は，皮膚や角膜などとともに再生医療のなかでも比較的臨床応用が進んでいる分野である。関節軟骨の局所的な欠損に対しては，非荷重部の関節軟骨から軟骨細胞を単離し，培養増殖させた後に細胞懸濁液として欠損部に投与する自家軟骨細胞移植（autologous chondrocyte implantation: ACI）

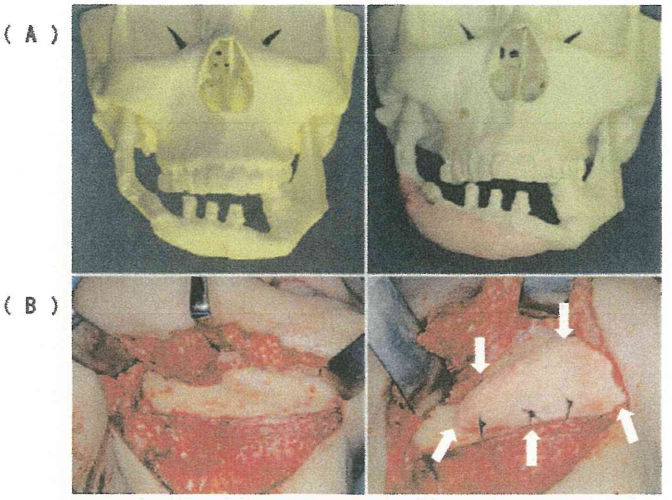

図 1　カスタムメイド人工骨（CT bone）
30 歳女性。下顎再建後の下顎変形に対し，リン酸三カルシウム粉体積層造形法により作製した CT bone を移植した。
(A) 三次元造形モデルを利用した CT bone のデザイン
(B) 右側下顎欠損部の陥凹部に移植された CT bone（矢印）。固定は吸収糸を用いて行った。

が，欧米を中心に医療として普及している[9]。しかしその適応範囲は依然として限局的で，層剥離，骨膜パッチの肥厚やグラフト逸脱などの問題点も指摘されている。また，既存の治療法と比較した際に，明らかな臨床上の優位性が認められないなど治療成績の限界も報告されている。顎顔面領域においても，隆鼻術後のシリコンインプラント抜去例や鞍鼻などに対して，患者の軟骨組織から単離した軟骨細胞を増殖培養させた後，皮下ポケットなどに注入して皮下再生軟骨を得るという方法が報告されている[10]。

このように，現行の軟骨再生医療は局所的な軟骨欠損の補填を目的とするため，移植される細胞は液状あるいはゲル状であり，膝関節の荷重に十分耐えうるような，あるいは顎顔面領域に適応可能な三次元形状を有する軟骨組織の再生は望めない。従って，軟骨再生医療の適応を，重度な軟骨損傷を伴う変形性関節症や顎顔面領域の先天性形態異常などへ拡大していくためには，力学的強度と適切な三次元形状を有する再生軟骨の開発が必要となる。そこでわれわれは，再生医療の 3 要素，すなわち細胞，成長因子，足場の観点から詳細な検討をすすめ，口唇口蓋裂に伴う重度の鼻変形（唇裂鼻変形）に適応可能なインプラント型再生軟骨の開発に取り組んできた。

細胞としては，軟骨組織由来の軟骨細胞，組織幹細胞に分類される種々の細胞のほか，胎生幹細胞（ES 細胞）あるいは人工多能性幹細胞（iPS 細胞）などが候補となりうる。このうち，①細胞培養により旺盛に増殖する[11]，②移植後自然に成熟する，③免疫拒絶や癌化のリスクが低い，④採取が比較的容易である，⑤倫理的に特に問題とならない，という特性を有する自家耳介軟骨細胞の活用が実用的であると判断した。成長因子に関しては，医薬品として既に安全性が確立されている 12 種類の成長因子・ホルモン（FGF-2，IGF-I，insulin，BMP-2 など）の組み合わせを，統計学的手法 fractional factorial design を用いて最適化し，ヒト軟骨細胞を 3 週間で 1000 倍程度増殖させる増殖培養液を開発した（ヒト血清および FGF-2/insulin 含有培養液 HFI）[12]。また，足場には，医療用生分解性ポリマーとして既に臨床応用されているポリ乳酸（poly-L-lactic acid:

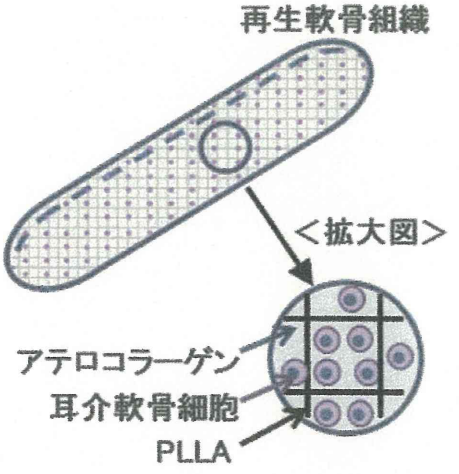

図 2　インプラント型再生軟骨

PLLA）やポリグリコール酸（poly-glycol acid: PGA）に関して形状検討を行い，アテロコラーゲンゲルとPLLA多孔体を組み合わせた足場素材複合体を開発した[13,14]。これらの知見を組み合わせることにより，生理的軟骨組織に匹敵する力学的強度を有するインプラント型再生軟骨の作製に成功した（図2）。大型動物を用いた前臨床試験において有効性と安全性を確認し，厚生労働省「ヒト幹細胞を用いる臨床研究に関する指針」に基づいて，学内臨床研究審査員会および厚生科学審議会の審議を経て，平成23年3月に厚生労働大臣の同意ならびに機関承認を受けた。現在，口唇鼻変形患者に対し，インプラント型再生軟骨の自主臨床研究を行っている（予定症例数3）。

V．将来展望

われわれが開発に携わってきた骨軟骨再生医療も，ようやく臨床応用段階に入ってきた。今後さらに汎用化，産業化を促し，再生医療を一層躍進させるためには，細胞培養に伴う複雑な製造工程を単純化することが望ましい。とはいえ，自己修復力に乏しい軟骨組織，関節組織の修復・再建，あるいは自然修復が困難な大型骨欠損に対しては，細胞を投与しなければ治癒は見込まれず，組織再生・再建のための細胞投与は必要不可欠であると考える。そこでわれわれは，細胞増殖と組織複合化の機能を再生組織の足場素材に集約・内蔵し，細胞プロセッシングセンターにおける製造工程を再現するような仕組みを再生組織そのものに組み込む技術開発を行っている（独立行政法人新エネルギー・産業技術総合開発機構　健康安心イノベーションプログラム，平成22-26年度）。これにより，再生医療製品に伴う複雑な製造工程の簡素化や培養期間の短縮化が実現すれば，品質の安定化と製品の普及に繋がるため，再生医療の新たな時代を築くことができるのではないかと期待している。

文　献

1) Langer R, Vacanti JP: Tissue engineering. Science 260：920-926, 1993.
2) 森　良之，高戸　毅：下顎再建における骨延長術の応用．口腔腫瘍，22：145-148，2010.
3) Iino M, Fukuda M, Nagai H, et al: Evaluation of 15 mandibular reconstructions with Dumbach Titan Mesh-System and particulate cancellous bone and marrow harvested from bilateral posterior ilia. Oral Surg Oral Med Oral Pathol Oral Radiol Endod 107：e1-8, 2009.
4) 飯野光喜，森　良之，近津大地，他：再生医学のいま　基礎研究から臨床への展開に向けて　In vivo tissue engineeringによる下顎骨再建．治療，91：2311-2315，2009.
5) 飯野光喜，森　良之，近津大地，他：『骨・軟骨の再生医療UPDATE』In vivo tissue engineeringによる顎骨再建の実際．Clinical Calcium，18：1757-1766，2008.
6) 鄭　雄一：インクジェットプリンターによるカスタムメイド人工骨．内分泌・糖尿病・代謝内科，32：305-310，2011.
7) 井川和代，望月　学，杉森　理，他：三次元インクジェットプリンターにより直接的に組み立てたテーラーメイドリン酸三カルシウム骨インプラント．人工臓器，37：14-16，2008.
8) Saijo H, ChungUng-Il, Igawa K, et al: 顎顔面における人工骨の臨床応用．J Artifi Org　11：171-176, 2008.
9) Marlovits S, Trattnig S: Cartilage repair. Eur J Radiol　57：1-2, 2006.
10) Yanaga H, Yanaga K, Imai K, et al: Clinical application of cultured autologous human auricular chondrocytes with autologous serum for craniofacial or nasal augmentation and repair. Plast Reconstr Surg 117：2019-2030, 2006.
11) Asawa Y, Ogasawara T, Takahashi T, et al: Aptitude of auricular and nasoseptal chondrocytes cultured under a monolayer or three-dimensional condition for cartilage tissue engineering. Tissue Eng Part A　15：1109-1118, 2009.
12) Takahashi T, Ogasawara T, Asawa Y, et al: Three-dimensional microenvironments retain chondrocyte phenotypes during proliferation culture. Tissue Eng 13：1583-1592, 2007.
13) Yamaoka H, Tanaka Y, Nishizawa S, et al: The application of atelocollagen gel in combination with porous scaffolds for cartilage tissue engineering and its suitable conditions. J Biomed Mater Res A　93：123-132, 2011.
14) Tanaka Y, Yamaoka H, Nishizawa S, et al: The optimization of porous polymeric scaffolds for chondrocyte/atelocollagen based tissue-engineered cartilage. Biomaterials　31：4506-4516, 2011.

Magn Reson Med Sci, Vol. 11, No. 1, pp. 27–34, 2012

MAJOR PAPER

Effects of Image Distortion Correction on Voxel-based Morphometry

Masami GOTO[1,2*], Osamu ABE[3], Hiroyuki KABASAWA[4], Hidemasa TAKAO[5], Tosiaki MIYATI[2], Naoto HAYASHI[6], Tomomi KUROSU[1], Takeshi IWATSUBO[7], Fumio YAMASHITA[8], Hiroshi MATSUDA[9], Sachiko INANO[5], Harushi MORI[5], Akira KUNIMATSU[5], Shigeki AOKI[10], Kenji INO[1], Keiichi YANO[1], and Kuni OHTOMO[5]; Japanese Alzheimer's Disease Neuroimaging Initiative

Departments of [1]Radiological Technology, [5]Radiology, and [6]Computational Diagnostic Radiology and Preventive Medicine, University of Tokyo Hospital
7–3–1 Hongo, Bunkyo-ku, Tokyo 113–8655, Japan
[2]Graduate School of Medical Science, Kanazawa University
[3]Department of Radiology, Nihon University School of Medicine
[4]Japan Applied Science Laboratory, GE Healthcare
[7]Department of Neuropathology, University of Tokyo
[8]Department of Radiology, National Center Hospital of Neurology and Psychiatry
[9]Department of Nuclear Medicine, Saitama Medical University International Medical Center
[10]Department of Radiology, Juntendo University
(Received April 27, 2011; Accepted August 31, 2011)

Purpose: We aimed to show that correcting image distortion significantly affects brain volumetry using voxel-based morphometry (VBM) and to assess whether the processing of distortion correction reduces system dependency.

Materials and Methods: We obtained contiguous sagittal T_1-weighted images of the brain from 22 healthy participants using 1.5- and 3-tesla magnetic resonance (MR) scanners, preprocessed images using Statistical Parametric Mapping 5, and tested the relation between distortion correction and brain volume using VBM.

Results: Local brain volume significantly increased or decreased on corrected images compared with uncorrected images. In addition, the method used to correct image distortion for gradient nonlinearity produced fewer volumetric errors from MR system variation.

Conclusion: This is the first VBM study to show more precise volumetry using VBM with corrected images. These results indicate that multi-scanner or multi-site imaging trials require correction for distortion induced by gradient nonlinearity.

Keywords: *brain volumetry, distortion correction, gradient field nonlinearities, magnetic resonance imaging, voxel-based morphometry*

Introduction

Voxel-based morphometry (VBM)[1] using 3-dimensional T_1-weighted (3D-T_1) magnetic resonance (MR) images has been employed to estimate local brain volume.[2–5] Previous studies investigated whether distortion might cause error in estimating brain volume and evaluated the accuracy of various methods for correcting distortion.[6–8] However, those reports did not investigate the effect of distortion correction with regard to computational brain volumetry analyses (i.e., boundary shift integral,[9] VBM,[1] tensor-based morphometry,[10] and atlas-based volumetry[11]). We agree that use of images corrected for distortion improves analysis but believe additional study is required of VBM that includes spatial normalization. This study has 2 aims. The first is to show that correcting distortion significantly affects brain volumetry using VBM. Because analytical procedures that include normalization may reduce the influence of distortion correction in VBM and obscure the effects of correction, it is important to confirm the need for correction in

*Corresponding author, Phone: +81-3-3815-5411, Fax: +81-4-7183-3337, E-mail: car6_pa2_rw@yahoo.co.jp

VBM. Following distortion correction, regions of increased volume would correspond to regions of reduced volume caused by distortion, and regions of reduced volume would correspond to those with increased volume caused by distortion.

Our second aim is to assess whether system dependency decreases in the processing of distortion correction. In multi-site studies, data obtained using different MR imaging systems are mixed in the same analytical flow. Consequently, previous reports of multi-site studies[12–14] showed less precise brain volumetry as a result of heterogeneous signal intensity and low signal-to-noise ratio (SNR). The degree of image distortion depends on such variables within the MR imaging system.[15] However, no reports have shown reduced volumetric precision of VBM as a result of using distorted images.

Materials and Methods

Subjects

Twenty-two healthy volunteers (17 men, 5 women; aged 23 to 47 years, mean age 31.1 ± 7.3 years) underwent MR imaging at 1.5 and 3 tesla, with 3D-T_1 images obtained the same day. A board-certified radiologist (O.A.) inspected the images and found none of the following in any subject: brain tumor, infarction, hemorrhage, brain atrophy, cognitive impairment, or white matter lesions graded higher than grade 2 of Fazekas classification.[16] Cognitive impairment was screened with a mini-mental state examination, and T_2-weighted images were used to evaluate white matter lesions. The ethical committee of our institution approved the study, and written informed consent was obtained from all participants.

MR imaging protocol

We obtained MR imaging data using 2 systems. The first was a 1.5T scanner (Signa EXCITE HD, GE Healthcare, Waukesha, WI, USA; 33 mT/m maximum strength, 120 T/m/s slew rate) with a quadrature head coil used for transmission and reception. We used 3D magnetization-prepared rapid gradient-echo (3D-MPRAGE) to obtain 184 contiguous sagittal T_1-weighted images with slice thickness, 1.3 mm; repetition time (TR)/echo time (TE), 3000 ms/3.9 ms; inversion time (TI), 1000 ms; flip angle, 8°; field of view (FOV), 24 cm; number of excitations (NEX), one; and matrix, 192 × 192 pixels. We used 2D fast spin-echo (2D-FSE) to obtain 48 axial T_2-weighted images with slice thickness, 3 mm; TR/TE, 3000 ms/100 ms; echo train length, 16; FOV, 24 cm; NEX, one; and matrix, 256 × 256 pixels.

The second system was a 3T scanner (Signa EXCITE HDx, GE Healthcare; 40 mT/m maximum strength, 150 T/m/s slew rate) with a quadrature head coil used for transmission and reception. We used 3D-MPRAGE to obtain 170 contiguous sagittal T_1-weighted images with slice thickness, 1.3 mm; TR/TE, 2300 ms/2.8 ms; TI, 900 ms; flip angle, 8°; FOV, 26 cm; NEX, one; and matrix 256 × 256 pixels. We used 2D-FSE to obtain 48 axial T_2-weighted images with slice thickness, 3 mm; TR/TE, 3000 ms/97 ms; echo train length, 16; FOV, 24 cm: NEX, one; and matrix, 256 × 256 pixels. We employed scanning protocols using the protocol of the Alzheimer's Disease Neuroimaging Initiative.

Image preprocessing for VBM

We used Statistical Parametric Mapping 5 (SPM5)[17] software for volumetric analysis, nonparametric nonuniform intensity normalization (N3) software[18] for intensity bias correction, and spherical harmonics description of gradients (SHDG)[8] for gradient nonlinearity distortion correction. Image distortion in MR has 6 potential sources-scale errors (linear) in gradient fields, shimming anomalies of the main magnet, chemical shift, B_0 eddy currents, nonlinearities of gradient fields, and magnetic susceptibility variations in various anatomical structures.[19] We can correct nonlinearities of gradient fields and know their influence is large, but we cannot correct magnetic susceptibility variations in anatomical structures. Therefore, we focused only on image distortion caused by nonlinearities of gradient fields.

The various distortion correction methods include SHDG, phase mapping,[20] adoption of a specially constructed phantom,[21] and the use of 2 frequency-encoding gradients.[22] We employed SHDG correction for nonlinearities of the gradient fields using the same method described by Jovicich and colleagues,[8] which employs information based on the design of the gradient coils; we used MR-specific information, such as the gradient correction coefficients. SHDG correction can correct image distortion caused by nonlinearities of the gradient fields but not distortion caused by other factors, such as magnetic susceptibility variations in various anatomical structures. Jovicich's group[8] reported the efficiency of SHDG correction in a study that showed distorted areas using a grid phantom and differences in brain surface boundaries using images of the human brain. Therefore, we further evaluated this method for VBM that included normalization.

We processed 3D-MPRAGE images with and without SHDG correction in SPM5 after N3 proc-

essing. In SPM5, 3D-MPRAGE images in native space were bias-corrected, spatially normalized, and segmented into images (i.e., gray matter, white matter, and cerebrospinal fluid); voxel size of the spatially normalized images was $2\times2\times2$ mm. We changed the affine regularization space template in the International Consortium for Brain Mapping from the European to the East Asian brain template. In the modulation step, we multiplied the voxel values of the spatially normalized gray and white matter images by a measure of the relative volumes of the warped and unwarped structures that were derived from the nonlinear step of spatial normalization (Jacobian determinant).

For each subject, we added the spatially normalized image of gray matter and that of white matter and defined this as the brain image in this study. Spatially normalized brain images were smoothed with 8-mm isotropic Gaussian kernels. Four sets of each processed volume were obtained as follows: (A) brain images with SHDG correction obtained with the 1.5T system; (B) brain images without SHDG correction obtained with the 1.5T system; (C) brain images with SHDG correction obtained with the 3T system; and (D) brain images without SHDG correction obtained with the 3T system.

To test for a statistically significant effect of distortion correction, we prepared differential images (DI). DI-1.5 was defined as (brain image with SHDG correction obtained with the 1.5T system)−(brain image without SHDG correction obtained with the 1.5T system). In statistical analysis of DI-1.5 for the 22 subjects, we assessed the effect of SHDG correction.

To investigate reduction in system dependency, we prepared DI-C and DI-nonC: DI-C was defined as (brain image with SHDG correction obtained with the 1.5T system)−(brain image with SHDG correction obtained with the 3T system), and DI-nonC was defined as (brain image without SHDG correction obtained with the 1.5T system)−(brain image without SHDG correction obtained with the 3T system). In statistical analysis of DI-Cs and DI-nonCs of the 22 subjects, we assessed whether SHDG correction resulted in fewer volumetric errors caused by variation in MR system.

Statistical analyses for the effect of distortion correction

We compared estimated brain volumes with and without SHDG correction using the DI-1.5s of the 22 subjects and analyzed the DI-1.5s with SPM5, employing the framework of the general linear model. To test hypotheses with respect to regionally specific group effects, we tested the estimates with one-sample t-test using VBM. In this analysis, "plus regions" were regions increased by SHDG correction, and "minus regions" were regions reduced by SHDG correction. The significance of each region was estimated by distributional approximations from the random Gaussian fields theory. $P<0.05$, corrected with family-wise error (FWE) in voxel difference and cluster size greater than 30 voxels, was considered statistically significant.

Statistical analyses for reduction of system dependency

We examined whether SHDG correction could reduce brain volumetric errors caused by MR system variation. We analyzed the DI-Cs and DI-nonCs of the 22 subjects using SPM5, employing the framework of the general linear model. To test hypotheses with respect to regionally specific group effects, we compared estimates with 2 linear contrasts using VBM. Correction of image distortion by SHDG indicated significant difference between DI-C and DI-nonC. The significance of each region was estimated by distributional approximations from the theory of random Gaussian fields. $P<0.05$, corrected with FWE in voxel difference and cluster size greater than 30 voxels, was considered statistically significant.

We prepared 2 design matrices to estimate system dependence in regions increased or reduced by nonlinearities of gradient fields. We used the first matrix (Fig. 3) to investigate system dependence inside regions reduced by SHDG correction. In analysis using this matrix, we estimated significant minus regions in the DI-nonC of the 22 subjects by VBM (uncorrected $P<0.05$) and set these minus regions as an inclusive mask. These significant minus regions indicated that volume expansion caused by nonlinearities of gradient fields was greater in the 3T system than the 1.5T system.

We used the second matrix (Fig. 4) to investigate system dependence within regions increased by SHDG correction. In analysis using this matrix, we estimated significant plus regions in the DI-nonC of the 22 subjects by VBM (uncorrected $P<0.05$) and set these plus regions as an inclusive mask. These significant plus regions indicate that volume reduction caused by nonlinearities of gradient fields was greater in the 3T system than the 1.5T system.

Results

Results of comparison between images with and without SHDG correction

Various regions of the brain showed significantly reduced (Fig. 1) and increased (Fig. 2) volumes fol-

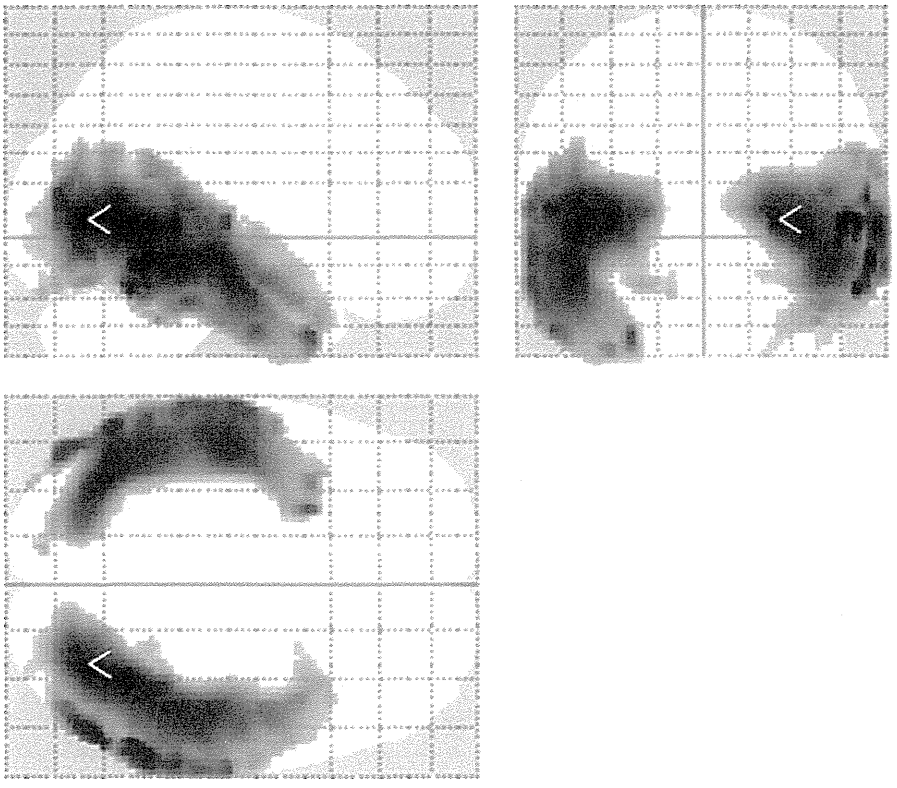

Fig. 1. The figure is a "glass brain" that indicates all regions in which brain volume was significantly reduced on corrected images compared to those without correction (gray scale, voxel with maximum effect indicated by red pointer). $P<0.05$, corrected with family-wise error (FWE) in voxel difference and cluster size greater than 30 voxels, was considered statistically significant.

lowing SHDG correction. Figure 1 shows all regions in which corrected images demonstrated significantly reduced local brain volume compared with uncorrected images. The Montreal Neurological Institute (MNI) coordinates of local maxima were 28, −70, 6 ($P<0.001$, T value = 14.97, cluster size = 12597). Figure 2 shows all regions in which corrected images demonstrated significantly increased local brain volume compared uncorrected images. MNI coordinates of local maxima were 22, 4, 54 ($P<0.001$, T value = 21.61, cluster size = 24441).

Results of brain volumetry error caused by MR system variation

SHDG correction decreased the system dependence of estimated brain volumes. Figure 3 shows all regions in which DI-nonC using uncorrected images had significant minus regions in comparison with DI-C using corrected images. In other words, brain volumetry was more system dependent using uncorrected images than corrected images; SHDG correction decreased system dependence within regions reduced by correction. MNI coordinates of local maxima were −46, −28, −12 ($P<0.001$, T value = 12.38, cluster size = 5573). Figure 4 shows all regions in which the DI-nonC of uncorrected images demonstrated significant plus regions in comparison with the DI-C of corrected images. In other words, brain volumetry was more system dependent using uncorrected images than corrected images; SHDG correction reduced system dependence within regions increased by correction. MNI coordinates of local maxima were −18, −8, 50 ($P<0.001$, T value = 10.07, cluster size = 7727). Figure 5 shows T_1WI with and without SHDG correction for a single subject.

Discussion

In our VBM study, we detected areas whose volumes increased or reduced by image distortion caused by nonlinearities of the gradient fields. Volume was reduced in the area around the temporal lobe and increased in the area around the frontal and parietal lobes. Thus, the influence of image distortion extends to the deep regions of the brain as well as surface regions. The results of com-

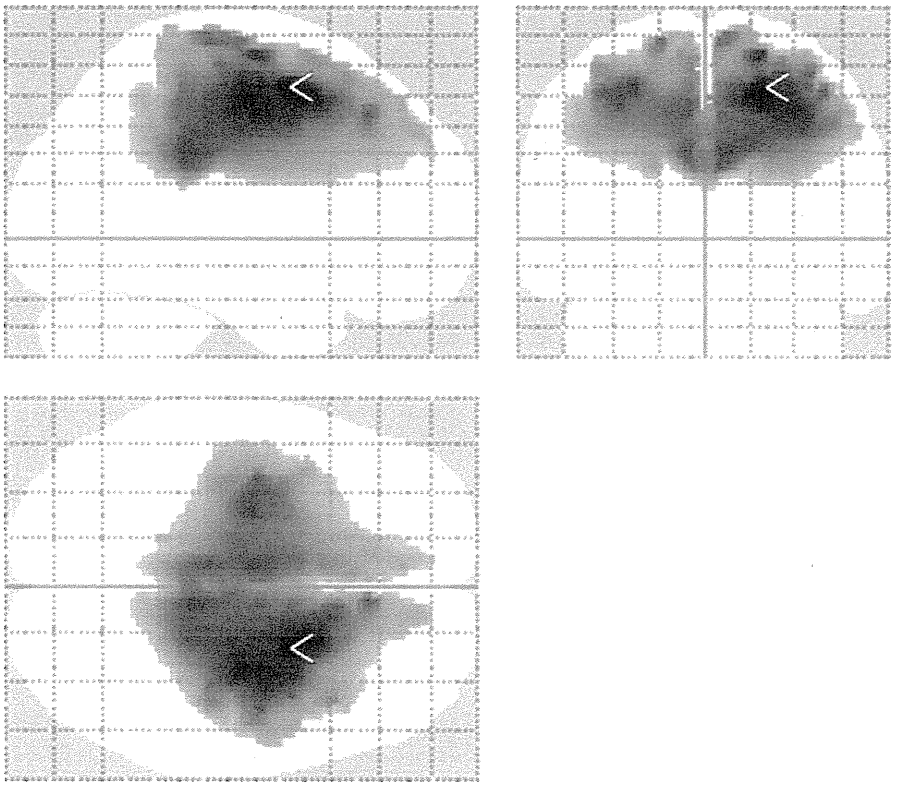

Fig. 2. The figure is a "glass brain" that indicates all regions in which brain volume was significantly increased on corrected images compared to those without correction (gray scale, voxel with maximum effect indicated by red pointer). $P<0.05$, corrected with family-wise error (FWE) in voxel difference and cluster size greater than 30 voxels, was considered statistically significant.

parison between corrected and uncorrected images (Figs. 1, 2) seem to deviate from the orthogonal frame of the gradients because the axis of the figures deviates from that frame; the images were obtained with most subjects lifting their chins against that frame. Therefore, we think that the areas of significant difference in our results are distributed according to the orthogonal frame of the gradients. The present study is the first to clarify the effect of SHDG correction on VBM.

McRobbie and associates showed that the amount of image distortion differs for each system.[15] Because distortion influences the results of VBM analysis, we considered the distortion to be related to system dependence. Therefore, we assessed whether image distortion correction processing resulted in reduced system dependency. The results (Figs. 3, 4) showed that SHDG correction reduced system dependency. Unfortunately, this result does not prove that distortion correction completely eliminates system dependency, but it does provide insight into the need for correcting image distortion in multi-site studies. Even in a study using a single system, image distortion affects analytical results because spatial placement of the main magnetic field center and the brain center influences the deformation volume due to distortion. This spatial placement in imaging differs among subjects.[8] In addition, the use of image distortion correction is strongly recommended in multi-site studies to minimize volumetric errors caused by system variation. In many institutions, however, VBM researchers may not always have access to MR-specific information or vendor-specific technical information, such as the gradient correction coefficients that should be used to perform SHDG correction. Therefore, previous studies may have utilized VBM studies using uncorrected images.

The major limitation of our study is that we cannot know the true brain volume. Neither can we explain whether the SHDG method performed excessive correction in this study. Therefore, we could demonstrate only that in brain volumetry using VBM, volume differed between SHDG-corrected and noncorrected images, and volumetry error due to system variation was decreased when image distortion correction was employed. Unfortunately, we could not show that VBM analysis with distor-

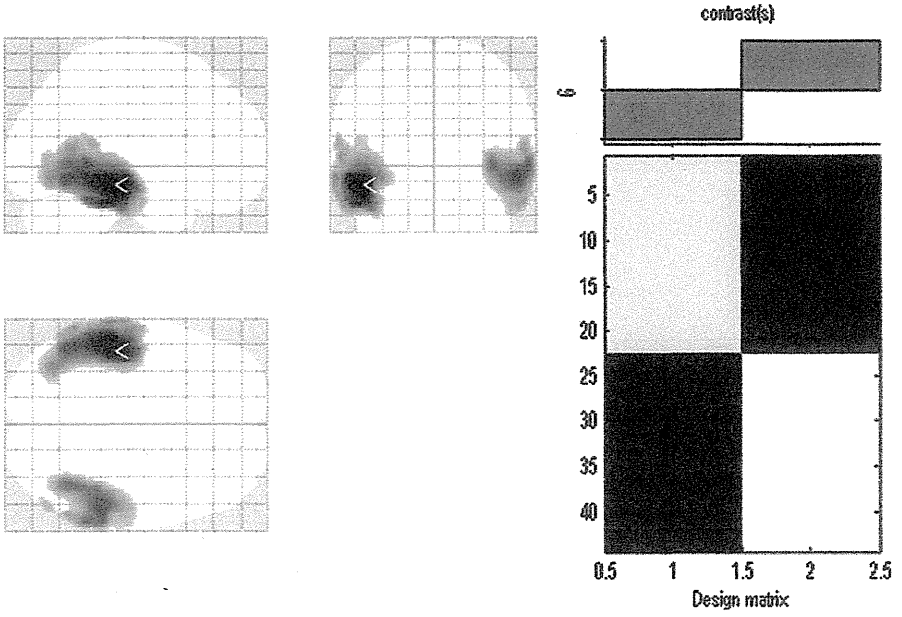

Fig. 3. Left side, a "glass brain" that indicates all regions in which system dependence was significantly less in corrected images than uncorrected images (gray scale, voxel with maximum effect indicated by red pointer). This figure showed system dependence inside increased regions caused by image distortion. Right side, design matrix. The left group in the design matrix comprised differential images (DI)-nonC and the right group, DI-C. P value < 0.05, uncorrected in voxel difference and cluster size greater than 30 voxels, was considered statistically significant.

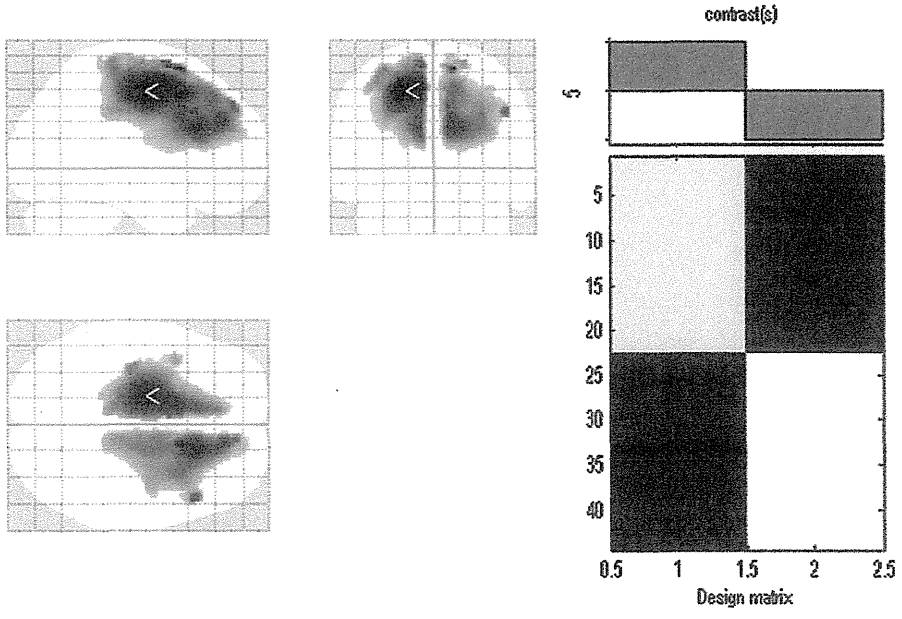

Fig. 4. Left side, a "glass brain" that indicates all regions in which system dependence was significantly less in corrected images than uncorrected images (gray scale, voxel with maximum effect indicated by red pointer). This figure showed system dependence inside reduced regions caused by image distortion. Right side, design matrix. The left group in the design matrix comprised differential images without correction (DI-nonC) and the right group, those with correction (DI-C). $P < 0.05$, uncorrected in voxel difference and cluster size greater than 30 voxels, was considered statistically significant.